New Ways to High-Quality Bulk Scandium Nitride

Rainer Niewa,* Dmitry A. Zherebtsov, Martin Kirchner, Marcus Schmidt, and Walter Schnelle

Max-Planck-Institut für Chemische Physik fester Stoffe, Nöthnitzer Strasse 40, 01187 Dresden, Germany

Received August 12, 2004. Revised Manuscript Received September 23, 2004

ScN was prepared in three different ways leading to single phase samples with low oxygen content in a broad range of particle sizes. Synthesis from the elements provides, in an exothermic reaction, brownish transparent single crystals (rock-salt structure type, space group $Fm\bar{3}m$, $a = 451.2(1)$ pm, $Z = 4$, $R_{int} = 0.034$, $R1 = 0.013$, $wR2 = 0.018$). From a decomposition reaction of $Li_3[ScN_2]$ fine brown powders (particle size $\approx 1\ \mu$m) were obtained. Via nitridation of intermetallic Sc−In phases even nanoscaled (<200 nm) ScN can be produced. The emerging In was converted to InI_3 and removed at comparable low temperatures ($T_{max} = 453$ K) by sublimation or extraction. Thermodynamic considerations enlighten the process. Crystal structure refinements, density measurements, and chemical analyses show an atomic ratio close to the ideal composition ScN with only a small vacancy concentration in the N-sublattice for all samples. Still, metal-like behavior in the electrical resistivity was observed (($\rho(300\ K) - \rho_0 = 1.1 \times 10^{-4}$ Ωcm, temperature coefficient $2.7 \times 10^{-3}\ K^{-1}$). This interpretation is in accordance with the magnetic susceptibility (temperature-independent paramagnetism $\chi_0 \approx 4 \times 10^{-6}$ emu/mol) and the observed band gap of $\Delta E = 2.10(2)$ eV. The oxidation behavior dependence on the particle size is analyzed.

1. Introduction

Within the last couple of years ScN has attracted several investigations because of its hardness, semiconducting properties, and possible use as an additive for ceramics to improve materials properties. For preparation of scandium nitride different techniques were employed: gray-black or blue samples were obtained by direct reaction of Sc with nitrogen gas,[1] Sc with ammonia,[2] or scandium hydride with ammonia[3] at comparably high temperatures up to 1770 K. Unfortunately, the kinetics of the reaction of Sc with nitrogen or ammonia is slow and may result only in nitrogen deficient products with bulk compositions ScN_x and x depending on T.[2] Early attempts to prepare ScN also included the reaction of Sc_2O_3 with carbon in nitrogen atmosphere,[4,5] but the products contained significant amounts of oxygen and/or carbon. Epitaxial growth was demonstrated from the reaction of volatile scandium halides with ammonia gas.[6] At lower temperatures of 673 K bulk ScN can be produced by thermal decomposition of the precursor $[ScCl_2\{N(SiMe_3)_2\}(THF)_2]$.[7] The red product is crystalline (unit cell parameter $a = 440(6)$ pm). Unfortunately, most samples produced or studied in such reports were only scarcely characterized in terms of composition and physical properties. This can be seen, e. g., in the range of unit cell parameters reported for ScN ($440\ pm \le a \le 451$ pm)[1,7,8] and the largely different data on the homogeneity range of ScN_x (e. g., for bulk samples, $0.87 \le x \le 1.00$,[1] $0.71 \le x \le 1.00$,[2] $0.74 \le x \le 0.87$;[9] for thin layers, no homogenity range[10]). A large and variable degree of vacancies on the nitrogen site may also account for a high electrical conductivity and the very different colors of the samples described in the literature as ranging from black and gray to red. These findings may similarly be due to impurities and incomplete conversion of Sc to ScN in the sense of two phase products.

Here, we present several new preparative routes to bulk ScN within a broad range of particle sizes such as fine powders with particle sizes smaller than 200 nm and single crystals of up to 1 mm. We characterize the products by thermal analyses, X-ray diffraction, chemical analysis, optical spectroscopy, density, magnetization, and electrical resistivity measurements.

2. Experimental Section

2.1 Handling and Methods. Since some of the substances in this study are air and moisture sensitive, and products with low oxygen contamination are considered of utmost importance, all manipulations were carried out in an argon-filled

* Corresponding author. Tel: +49 (0) 351 4646 3205. Fax: +49 (0) 351 4646 3002. E-mail: niewa@cpfs.mpg.de.

(1) Lengauer, W. *J. Solid State Chem*. **1988**, *76*, 412.
(2) Lyutaya, M. D.; Goncharuk A. B.; Timofeeva, I. I. *Tranl. Zh. Prikl. Khim.* **1975**, *48*, 721.
(3) Wilkenson, M. K.; Child, H. R.; Cable, J. W.; Wollan E. O.; Koehler, W. C. *J. Appl. Phys. Suppl*. **1960**, *31*, 358.
(4) Friedrich E.; Sittig, L. *Z. Anorg. Allg. Chem*. **1925**, *143*, 4.
(5) Samsonov, G. V.; Lyutaya M. D.; Neshpor V. S. *Zh. Prikl. Khim*. **1962**, *36*, 2108.
(6) Dismukes, J. P.; Yin W. M.; Ban V. S. *J. Cryst. Growth* **1972**, *13/14*, 365.
(7) Karl, M.; Seybert, G.; Massa W.; Dehnicke, K. *Z. Anorg. Allg. Chem*. **1999**, *625*, 375.
(8) Hajek, B.; Brozek V.; Duvigneaud, P. H. *J. Less-Common Met.* **1973**, *33*, 385.
(9) Aivazov, M. I.; Rezchikova T. V.; Gurov, S. V. *Izv. Akad. Nauk SSSR, Neorg. Mater.* **1977**, *13*, 1235.
(10) Porte, L. *J. Phys. Chem.: Solid State Phys*. **1985**, *18*, 6701.

10.1021/cm048667y CCC: $27.50
Published on Web 11/11/2004

glovebox ($p(O_2, H_2O) < 1$ ppm). All gases (Ar, N_2, Messer-Griesheim, 99.999%) used for the reactions were additionally purified by passing over molecular sieve (Roth 3 Å) and BTS-catalyst (Merck).

Elemental analyses on oxygen, carbon, and nitrogen were carried out using the hot-extraction technique on a LECO analyzer TC-463 DR. Quantitative analyses of Li and Sc were performed using an ICP−OES (Varian Vista RL).

The binary and ternary nitride products were characterized by X-ray powder diffraction using an imaging plate Guinier camera (HUBER diffraction, Cu $K\alpha_1$ radiation, 4 × 15 min scans, $8° \leq 2\Theta \leq 100°$). In each case, the sample was loaded between two polyimide foils in an aluminum cell with a rubber seal to exclude moisture. Unit cell parameters were refined by least-squares fits of X-ray powder data (CSD program package)[11] with LaB_6 as an internal standard ($a = 415.7$ pm). X-ray diffraction intensity data of a single crystal (0.1 mm × 0.1 mm × 0.05 mm sealed in a glass capillary) were collected on a MSC−Rigaku CCD applying Mo Kα radiation.

Simultaneous thermoanalytic and thermogravimetric measurements (DTA/TG) were performed on a STA 449C (Ar- or N_2-atmosphere purified as described above, Ni-crucibles, thermocouple type S, NETZSCH) completely integrated into a glovebox to avoid any hydrolysis or oxidation of the samples. Temperature calibration was obtained using 5 melting standards in the temperature range of 370−1470 K.

The optical band gap was determined from diffuse reflectance (Cary 500, praying mantis, white standard $BaSO_4$, ratio 5:1) under inert conditions. The absorption edge was taken as the inflection point of the steplike decrease of the diffuse reflectivity.

A SQUID magnetometer (Quantum Design MPMS-XL 7, temperature range 1.8−400 K) was used for magnetic susceptibility measurements in different magnetic fields. The samples were sealed in silica tubes under helium atmosphere (p(He) = 400 mbar). Only corrections for the sample containers were applied.

Four-point dc electrical resistivity measurements were performed on a single crystal ($1.2 \times 0.9 \times 0.9$ mm^3) in the temperature range 3.8−320 K. Four Cu wires were attached to the crystal with Ag-filled epoxy, and the assembly was mounted in a cryostat fully integrated in an Ar-filled glovebox.

For the determination of the bulk density the volume of a known sample mass was measured in a helium gas pycnometer (AccuPyc 1330, Micromeritics).[12]

The morphology and size distribution of the ScN powder were examined by scanning electron microscopy (SEM, Philips XL30, EDX detector).

2.2 Preparation. *2.2.1 Synthesis from the Elements.* Sc metal (Hunan Institute of Rare-Earth Metals Materials, China; sublimed, dendritic, chemical analyses w(O) = 0.09(2) %, w(N, C) below detection limit ≪0.01%) was heated in a nitrogen atmosphere within an induction furnace (Hüttinger TIG 5/300, W-crucible) to 1670 K, held at this temperature for 2 h, and cooled naturally by switching off the current. By grinding the product powder bulk material can be produced. With faster heating rates the sample may partially melt, probably due to the additional heat of the reaction. In such a way, single crystals with edge sizes up to 1 mm could be obtained from the melt (Figure 1). The crystals and the powder are dark brown, while thin edges of the single crystals are translucent reddish-brown. The characterization of the microcrystalline sample and the single crystals via XRD, density measurements, and chemical analyses led to the following data.

Microcrystalline Sample. Cubic unit cell parameter a = 450.79(1) pm, $Z = 4$, experimentally obtained density $\rho_{exp.}$ = 4.254(1) g/cm^3 ($\rho_{x\text{-ray}}$ = 4.276(1) g/cm^3 from unit cell parameter and the composition ScN). Results from chemical analyses: w(Sc) = 76.4(7)%, w(N) = 23.3(6)%, w(O) = 0.19(6)%, i.e., $Sc_{1.00(1)}N_{0.98(2)}O_{0.007(2)}$.

Single Crystals. Cubic unit cell parameter a = 451.2(1) pm, $Z = 4$, experimentally obtained density $\rho_{exp.}$ = 4.28(2) g/cm^3 ($\rho_{x\text{-ray}}$ = 4.264(3) g/cm^3 from unit cell parameter and the composition ScN). Results from chemical analyses: w(Sc) = 77.4(5)%, w(N) = 23.1(2)%, w(O) = 0.15(3)%, i.e., $Sc_{1.000(6)}N_{0.960(6)}O_{0.005(1)}$.

Figure 1. Photograph of ScN single crystals obtained from the reaction of the elements.

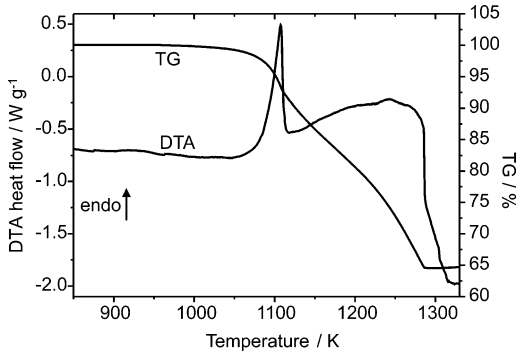

Figure 2. DTA/TG diagram of the decomposition of $Li_3[ScN_2]$ in Ar-atmosphere (heating rate 10 K/min).

2.2.2 Thermal Decomposition of $Li_3[ScN_2]$. $Li_3[ScN_2]$ was prepared as described elsewhere.[13] As established by DTA/TG measurements the ternary nitride decomposes above temperatures of 1120 K under evaporation of Li_3N to form ScN (dark brown, a = 450.35(2) pm). Figure 2 shows the simultaneous DTA/TG diagram in Ar atmosphere. The kink in the TG curve is probably due to melting of emerging Li_3N reducing the surface for sublimation.[13] The product of a sample heated to 1370 K for 10 h in nitrogen atmosphere has a typical composition of $Li_{0.022(1)}Sc_{1.00(1)}N_{1.021(4)}O_{0.018(2)}$ (chemical analyses: w(Li) = 0.255(2)%, w(Sc) = 75.1(8)%, w(N) = 23.89(9)%, w(O) = 0.48(4)%).

2.2.3 Reaction of Binary Intermetallic Compounds from the System Sc−In with Nitrogen. Intermetallic compounds (Sc_3In, Sc_2In, Sc_5In_3, ScIn, Sc_3In_5, or $ScIn_2$) were produced by arc-melting of In (99.9999% Chempur) and Sc in the corresponding molar ratios. Prior to the reactions with nitrogen, these samples were annealed in sealed quartz ampules at 1170 K. The general behavior of the intermetallic compounds with nitrogen gas was analyzed using DTA/TG measurements with T_{max} = 1370 K.

Samples ScN for characterization were obtained from reaction of $ScIn_x$ powders (typically ScIn, Sc_2In) with nitrogen at T = 1220 K (feasible at $T \geq 1120$ K) for 50 h.

(11) Akselrud, L. G.; Grin, Yu. N.; Zavalii, P. Y.; Pecharsky V. K.; Fundamenski, V. S. *Z. Kristallogr. Suppl.* **1989**, *2*, 155. Akselrud, L. G.; Zavalii, P. Y.; Grin, Yu. N.; Pecharsky, V. K.; Baumgartner B.; Wölfel, E. *Mater. Sci. Forum* **1993**, *133−136*, 335.

(12) Webb P. A.; Orr, C. *Analytical Methods in Fine Particle Technology*; Micromeritics Instruments Corp.: Norcross, GA, 1997.

(13) Niewa, R.; Zherebtsov D. A.; Leoni, S. *Chem. Eur. J.* **2003**, *9*, 4255.

Table 1. Crystallographic and Refinement Data for a Single Crystal of $ScN_{0.99(2)}$

compound	$ScN_{0.99(2)}$
crystal system	cubic
space group	$Fm\bar{3}m$ (No. 225)
unit cell parameter a [pm]	451.2(1)
V [10^6 pm^3]	91.86
Z	4
D_x [g cm^{-3}]	4.264
monochromator	graphite
μ(Mo Kα) [mm^{-1}]	6.88
absorption correction	empirical
Θ_{max} [deg]	34.23
h, k, l	−7−5, −6−6, −6−6
refl.	362
refl. unique	21
refl. $I \geq 2\sigma(I)$	21
R_{int}	0.034
Sc	0, 0, 0, $U_{iso} = 0.0050(2) \times 10^{-4}$ pm^2
N	$^1/_2$, 0, 0, $U_{iso} = 0.0069(9) \times 10^{-4}$ pm^2 occ. = 0.99(2)
refined parameters	4
GOF	0.995
R1, wR2 (all data)	0.013, 0.018
largest peak and hole in e^- difference map [Å^{-3}]	0.37, −0.34

2.2.4 Separation of ScN from In. The separation process of In from the ScN powder may proceed on different routes. Vacuum distillation of In is only feasible at comparably high temperatures and with comparably long heating periods depending on the sample mass. During this process ScN particles may grow—an undesired effect. An alternative separation process utilizes the high volatility of indium halides. The first step in the separation process of ScN from In is a reaction with I_2 at $T = 453$ K to obtain InI_3. For this reaction only a small excess of I_2 (~1 wt %) should be applied. The reaction is conducted in a sealed silica tube. For the sake of small particle sizes, this reaction as well as the subsequent separation process of InI_3 from ScN should be conducted at the lowest possible temperatures.

InI_3 might be sublimated in a temperature gradient from 433 to 323 K. This procedure might be directly carried out within the fused silica tube from the reaction with I_2. InI_3 can alternatively be sublimated in a dynamic vacuum at ambient temperature within 2 days. A further convenient way to remove InI_3 is the extraction with a water-free organic solvent. Useful solvents are, e.g., toluene and DMF. The purification process was carried out in a Soxhlet extractor within 2 h.

Analogous experiments with Br_2 instead of I_2 did not lead to single phase ScN. Formation of $ScBr_3$ next to $InBr_3$ was observed independent of the applied conditions.

A typical product composition from chemical bulk analyses is $ScN_{0.963(9)}O_{0.04(1)}In_{0.007(6)}Ta_{0.00072(5)}Al_{0.0055(2)}I_{0.005}$ (I was determined only half-quantitative), with Ta as a known impurity in Sc and Al traces originating from Al_2O_3 crucible material. The analyzed sample possesses a unit cell parameter of $a =$ 450.11(2) pm, typical values lie in the range of 499.9−450.1 pm with the smaller values for lower reaction temperatures.

3. Results and Discussion

3.1 Synthesis from the Elements. The products from the high-temperature preparation were characterized via X-ray powder diffraction, single-crystal X-ray structure refinements, chemical analyses, and density measurements. For the powder material from the unit cell $a = 450.79(1)$ pm a density of $\rho = 4.276(1)$ g/cm^3 calculates for the ideal composition ScN. The experimental density $\rho_{exp.} = 4.254(1)$ g/cm^3 indicates a small degree of vacancies. Assuming the occurrence of no other defects (e.g., of Frenkel type) except nitrogen deficiency, a composition of $ScN_{0.98}$ results from these values. This is in good agreement with the composition from chemical analyses: $ScN_{0.98}O_{<0.01}$. For the single crystals the data on the experimental density show a high uncertainty due to a small sample amount. Here, the composition from the single-crystal structure refinement of $ScN_{0.99(2)}$ should be more reliable (Table 1). Certainly, within this technique, it is not possible to differentiate between N and O at the site of the anions in the crystal structure, but the chemical analyses indicate an even lower content of O than for the powder material (see Experimental Section).

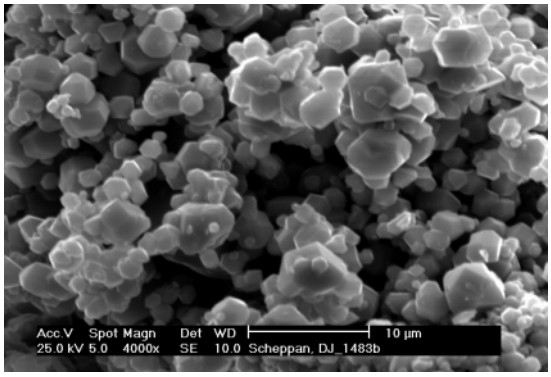

Figure 3. Scanning electron microscopy representation of ScN particles obtained from decomposition of $Li_3[ScN_2]$.

Single crystals of the binary nitrides RN of the more volatile rare-earth metals R = Gd, Ho, Dy, Tb, and Eu could be grown by sublimation in sealed molybdenum crucibles,[14−16] while EuN single crystals also were obtained from europium and potassium in supercritical ammonia at $T = 770$ K.[17] The single crystals ScN grown in the high frequency furnace from partly molten Sc are well-shaped cubes. The transparency of the thinner edges of such crystals (reddish-brown) indicates semiconducting behavior connected with a small concentration of defects in the sense of x in ScN_x near unity, as also indicated by the chemical analyses and the single-crystal X-ray diffraction data.

3.2 Synthesis from Decomposition of a Precursor. ScN powders were also prepared by thermal decomposition of the ternary precursor $Li_3[ScN_2]$. DTA/TG measurements indicate the reaction starts at about $T = 1100$ K (compare Figure 2). Samples fired for 1 h at $T = 1570$ K to obtain complete decomposition and elimination of emerging Li_3N revealed small amounts of remaining Li and particle sizes of about 1 μm (Figure 3). As might be expected, longer heating times lead to increasing particle sizes.

3.3 Synthesis from Intermetallic Phases. Binary nitride formation from metallic fluxes is currently under investigation due to the potential applications of binary nitrides as hard materials, for magnetic applications, and for removal of fission products from spent nuclear fuels.[18] Metallic fluxes typically used are mercury,[14,16,19−21] cadmium,[22] and tin.[18,23,24] These metals do not form binary nitrides under the applied conditions.

(14) Busch, G.; Kaldis, E.; Schaufelberger-Teker E.; Wachter, P. *Les Elements des Terres Rares*, Vol. I; Intern. du CNRS: Paris-Grenoble, May 1969; p 359.
(15) Busch, G.; Junod P.; Vogt, O. *Colloq. Int. Paris* **1967**, *157*, 337.
(16) Kordis, J.; Gingerich, K. A.; Seyse, R. J.; Kaldis E.; Bischof, R. *J. Cryst. Growth* **1972**, *17*, 53.
(17) Jacobs H.; Fink, K. *Z. Anorg. Allg. Chem*. **1978**, *438*, 151.
(18) Schicks, T.; Anderson R. N.; Parlee, N. A. D. *High Temp. Sci*. **1974**, *6*, 351.

Mercury and cadmium can be easily removed from the products by distillation. The drawbacks are environmental considerations for use of mercury and cadmium and the high boiling temperature for tin. Additionally, mercury might be incorporated in the nitride products as known for some transition metal systems.[19] With tin the formation of the binary phase Sn_3R was observed (R = rare-earth metal).[23] These intermetallics seem to be stable against nitridation for some rare-earth metals R and, thus, limit the yield of RN. For production of high-quality semiconducting binary RN_x phases with N contents close to unity low temperatures are required for the reaction as well as in the recovery process following the nitridation to minimize the degree of N vacancies in the product. The use of intermetallic compounds instead of molten alloys for reaction with gaseous nitrogen contains several advantages: it minimizes the amount of flux-metal (i.e., Sn, In) to be removed in a second step and reduces the temperature necessary for the reaction.

3.3.1 Reaction with Nitrogen. To gain a deeper insight into the ScN formation, the thermal behavior and reactivity of intermetallic compounds with different compositions from the binary phase diagram Sc−In were studied under the conditions of DTA/TG in N_2, O_2, and Ar atmosphere. Figure 4 gives some examples of the DTA/TG measurement curves. DTA/TG analyses of intermetallic compounds $ScIn_x$ in purified nitrogen atmosphere were performed for all known phases of the phase diagram:[25] Sc, Sc_3In, Sc_2In, Sc_5In_3, and Sc_3In_5. A recent revision of the phase diagram replaces Sc_5In_3 and Sc_3In_5 by ScIn and $ScIn_2$, respectively.[26] Under the reaction conditions of DTA/TG in nitrogen atmosphere pure Sc slowly starts to gain weight only above temperatures of 1220 K. Even after heating to 1470 K the accumulated weight gain typically is only $^1/_3$ of the expected value for full conversion to ScN. All intermetallic compounds except Sc_3In_5 react with nitrogen within a small temperature window to form fine powders of ScN and In (InN is not formed due to its marginal thermodynamic stability and the decomposition temperature of 773 K under $p(N_2) = 1$ bar).[27] Remarkably, the Sc-poorest intermetallic compound, Sc_3In_5, does not show any significant reaction with N_2 up to temperatures of 1470 K, even in the molten state ($T_{liq} \approx 1193$ K) well above its peritectic decomposition temperature (1186 K) and the liquidus. ScIn starts to react with N_2 at about 1220 K, while Sc_5In_3, Sc_2In, and Sc_3In already react at temperatures of about 1120 K (compare Figure 4a−c). Similar behavior was previously reported for La_3In and Dy_2In.[28]

In some DTA/TG measurements starting with Sc−In intermetallics, a step corresponding to the formation of cubic $(Sc_3N)In$[28] (according to X-ray powder diffraction diagrams of the rapidly cooled product mixture) was observed in the TG curve. This step was most prominent

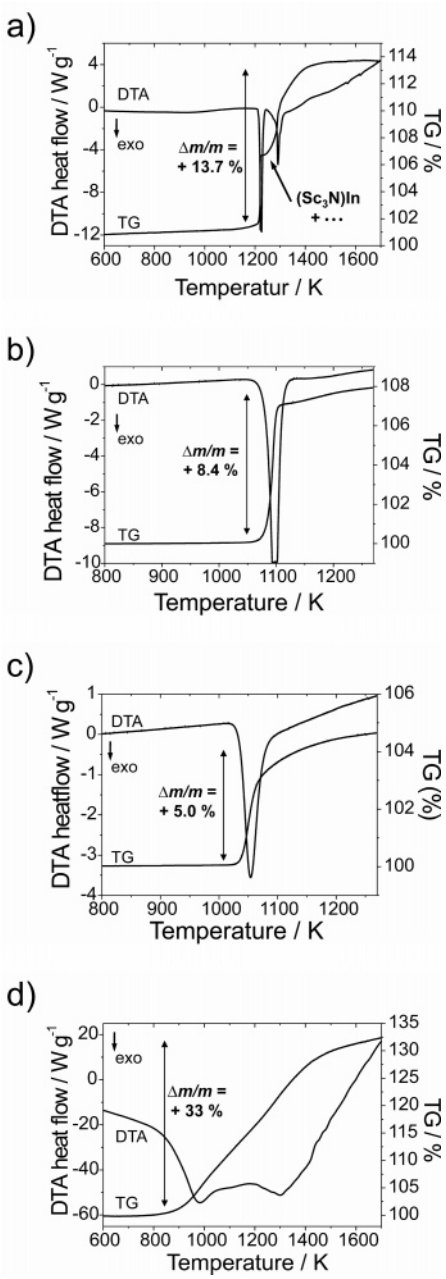

Figure 4. DTA/TG diagrams (heating rate 10 K/min) of the reaction of different binary intermetallic compounds: (a) Sc_2In, (b) ScIn, (c) $ScIn_2$ in nitrogen flow, and (d) Sc_2In in oxygen flow.

(19) Ettmayer, P. PhD thesis, Universität Wien, Vienna, Austria, 1964.
(20) Anderson R. N.; Parlee, N. A. D. *Metall. Trans*. **1971**, *2*, 1599.
(21) Magyar, B. *Inorg. Chem*. **1968**, *7*, 1457.
(22) Akabori, M.; Itoh A.; Ogawa, T. *J. Nucl. Mater*. **1997**, *248*, 228.
(23) Fuwa, A.; Anderson R. N.; Parlee, N. A. D. *High Temp. Sci*. **1973**, *5*, 165.
(24) Fuwa, A.; Anderson R. N.; Parlee, N. A. D. *High Temp. Sci*. **1973**, *5*, 325.
(25) Yatsenko, S. P.; Semyannikov, A. A.; Shakarov H. O.; Fedorova, E. G. *J. Less-Common Met.* **1983**, *90*, 95.
(26) Palenzona, A.; Manfrinetti P.; Palenzona, R. *J. Alloys Comp*. **1996**, *243*, 182.
(27) Onderka, B.; Unland J.; Schmid-Fetzer, R. *J. Mater. Res*. **2002**, *17*, 3065. Ranade, M. R.; Tessier, F.; Navrotsky, A.; Marchand, R. *J. Mater. Res*. **2001**, *16*, 2824.
(28) Kirchner, M.; Schnelle, W.; Wagner F. R.; Niewa, R. *Solid State Sci*. **2003**, *5*, 1247.
(29) Mulokozi, A. M. *J. Less-Common Met*. **1981**, *79*, 145.
(30) Miedema, A. R. *J. Less-Common Met*. **1976**, *46*, 67.
(31) Morita, Z.; Jung W. G.; Tanaka, T. *Trans. Jpn. Inst. Met.* **1987**, *28*, 232.
(32) Huber, E. J.; Fitzgibbon, G. C.; Head E. L.; Holley, C. E. *J. Phys. Chem*. **1976**, *67*, 1731.
(33) Barin, I. *Thermochemical Data of Pure Substances*; VCH: Weinheim, 1989.
(34) Nelson P. G.; Sharpe, A. G. *J. Chem. Soc. A* **1966**, 501.
(35) Oppermann, H. *Freiberger Forschungshefte A 767*; VEB Deutscher Verlag für Grundstoffindustrie: Leipzig, Germany, 1987; p 97.
(36) Kaldis, E.; Zürcher, Ch. *Rapp. Sess. Printemps Soc. Suisse Phys.* **1974**, *47*, 421.
(37) Schwarz, K.; Weinberger P.; Neckel, A. *Theor. Chim. Acta* **1969**, *15*, 153.
(38) Sclar, N. *J. Appl. Phys*. **1964**, *35*, 1534.

in reactions of Sc_2In with N_2 (Figure 4a). At higher temperatures or with longer dwelling times a mixture of ScN powder and In flux is obtained. This is in contrast to the reaction of pure Sc with nitrogen: the reaction is still slow above $T > 1500$ K and not completed when the melting point of Sc is reached (1812 K). Thus, the reaction leads to compact ScN and often incomplete reaction due to kinetic barriers. For comparison, the reaction of Sc_2In with pure O_2 significantly occurs already at about $T \approx 800$ K (compare Figure 4d). In contrast to the reactions with N_2 it conducts over a broad temperature range and is not completed, even at a maximum temperature of 1700 K. The reason is the formation of In_2O_3 instead of In metal next to Sc_2O_3 (and solid solutions $(In_{1-x}Sc_x)_2O_3$ of both isotypic binary oxides), thus leading to a diffusion-controlled reaction.

Similar reactions of intermetallic compounds and phases containing Ga instead of In also lead to low reaction temperatures and small particle sizes of the resulting ScN. However, impurities are an issue due to corrosion of the crucible by the emerging Ga; depending on the crucible material, Mo_2N, MoN, $ScNbN_2$, and $ScTaN_2$ were observed.

3.3.2 Separation of ScN from Flux Metal. In the following we discuss the separation process of ScN from flux-metal by a chemical route exemplarily for In. The separation of ScN and In was conducted via reaction with I_2 at $T = 453$ K and sublimation of the obtained InI_3 in a temperature gradient from 433 to 323 K. Similar experiments with Br_2 instead of I_2 led to formation of $ScBr_3$, while no ScI_3 was observed in the presence of I_2. The different involved processes can be explained with the available thermodynamic data of the reaction components as follows.

The calculations are based on the free enthalpies of formation for ScN and ScI_3 as obtained as averages of values of standard enthalpies and entropies from the literature:

The standard enthalpies of formation of ScN ($\Delta H_f(ScN_{s,298})$) obtained from theoretical considerations

$$\Delta H_f(ScN_{s,298}) = -311.37 \text{ kJ/mol}^{29}$$

$$\Delta H_f(ScN_{s,298}) = -359.82 \text{ kJ/mol}^{30}$$

$$\Delta H_f(ScN_{s,298}) = -343.60 \text{ kJ/mol}^{31}$$

lead to an average value of

$$\mathbf{\Delta} H_f(ScN_{s,298}) = -338 \text{ kJ/mol}$$

An experimentally obtained value from heats of solution is

$$\Delta H_f(ScN_{s,298}) = -313.8 \pm 16.7 \text{ kJ/mol}^{32}$$

In the following the average value from theory was used, since it better describes our experimental findings with the understanding, that the values for ScI_3 and $ScBr_3$ are considered well established. The standard entropy of ScI_3 is unknown, therefore we estimated it from the value of $ScBr_3$.

Using the standard entropy of ScN $S^0(ScN_{s,298}) = 29.706$ J/mol K and the tabulated C_p-values[33] one obtains a free energy for ScN of

$$\Delta G(ScN_{s,450}) = -353 \text{ kJ/mol}$$

For ScI_3 (s) the free energy was calculated analogously from

$$\Delta H_f(ScI_{3s,298}) = -523 \pm 12.5 \text{ kJ/mol}^{34}$$

and the standard entropy

$$S^0(ScI_{3s,298}) = -188.7 \text{ J/mol K}$$

(calculated from $1/x\, S^0(MI_x) = 1/x\, S^0(MBr_x) + 7.1$ J/mol K, and $S^0(ScBr_{3s,298}) = 167.360$ J/mol K).[33,35] Use of the tabulated C_p-values[33] of $ScBr_3$ (s) results in

$$\Delta G(ScI_{3s,450}) = -608 \text{ kJ/mol}$$

On the basis of these parameters, the free energies of the remaining components

$$\Delta G(In_{liq,450}) = -27.108 \text{ kJ/mol}^{33}$$

$$\Delta G(InI_{3s,450}) = -331.981 \text{ kJ/mol}^{33}$$

$$\Delta G(I_{2g,450}) = -56.229 \text{ kJ/mol}^{33}$$

$$\Delta G(N_{2g,450}) = -87.280 \text{ kJ/mol}^{33}$$

and the following reaction equations

$$2\,In\,(liq) + 3\,I_2\,(g) \rightarrow 2\,InI_3\,(s) \qquad \Delta G_{r,450} = -441 \text{ kJ/mol} \quad (1)$$

$$2\,ScN\,(s) + 3\,I_2\,(g) \rightarrow 2\,ScI_3\,(s) + N_2\,(g) \qquad \Delta G_{r,450} = -429 \text{ kJ/mol} \quad (2)$$

$$2\,ScN\,(s) + 2\,InI_3\,(s) \rightarrow 2\,ScI_3\,(s) + 2\,In\,(liq) + N_2(g) \qquad \Delta G_{r,450} = 12 \text{ kJ/mol} \quad (3)$$

the whole process can be described in the following way: in a first step the formation of InI_3 occurs as a kinetically controlled reaction. A reaction of ScN and I_2 to ScI_3 must be expected from the thermodynamic point of view, but was never observed. After the complete transformation of In to InI_3 the only products are ScN and InI_3. The hypothetical reaction of these compounds has a positive free energy of reaction, thus is not to be expected, and therefore InI_3 can be removed from ScN in a second step by sublimation. Starting from these calculations suitable conditions for both steps were derived as stated above. Experiments at temperatures above 453 K failed, because under these conditions the kinetically controlled reaction of iodine converts into a thermodynamically controlled reaction leading to the formation of large amounts of ScI_3. Similarly, temperatures above 433 K for the sublimation were ineffective, since the iodine partial pressure increases due to the decomposition equilibrium:

$$InI_3\,(liq) \rightleftarrows InI\,(liq) + I_2\,(g) \quad (4)$$

Analogous experiments with Br_2 instead of I_2 did not lead to single phase ScN. A formation of $ScBr_3$ next to $InBr_3$ was observed independent of the applied conditions. This is also easily explained considering the thermodynamic data and possible reactions

$$\Delta G(ScBr_{3s,450}) = -821.471\ \text{kJ/mol}^{33}$$

$$\Delta G(InBr_{3s,450}) = -512.959\ \text{kJ/mol}^{33}$$

$$\Delta G(Br_{2g,450}) = -80.835\ \text{kJ/mol}^{33}$$

$$2\ \text{In (liq)} + 3\ Br_2\ \text{(g)} \rightarrow 2\ InBr_3\ \text{(s)} \qquad \Delta G_{r,450} = -729\ \text{kJ/mol} \quad (5)$$

$$2\ \text{ScN (s)} + 3\ Br_2\ \text{(g)} \rightarrow 2\ ScBr_3\ \text{(s)} + N_2\ \text{(g)} \qquad \Delta G_{r,450} = -782\ \text{kJ/mol} \quad (6)$$

$$2\ \text{ScN (s)} + 2\ InBr_3\ \text{(s)} \rightarrow 2\ ScBr_3\ \text{(s)} + 2\ \text{In (liq)} + N_2\ \text{(g)} \qquad \Delta G_{r,450} = -52\ \text{kJ/mol} \quad (7)$$

The free energy of reaction of ScN with $InBr_3$ at T = 450 K is negative, therefore the kinetic control of the reaction of In with Br_2 cannot work as accurately as in the case of reaction with I_2 and, thus, $ScBr_3$ is formed.

3.4 Characterization of ScN. While the high temperature (exothermic, partially self-heated) direct synthesis leads to single crystals with edge sizes up to several mm, the decomposition route and the nitridation of intermetallics results in small particle sizes. The technique of nitridation of intermetallics with the lowest preparation and purification temperatures yields particles in the range below 200 nm (Figure 5) while the much higher temperatures of the decomposition (1570 K) in the decomposition process provides particle sizes of ≥ 1 μm. The oxidation behavior of ScN powders of different particle sizes was analyzed using simultaneous DTA/TG. For separation of particle size ranges the ScN sample from the conventional high-temperature synthesis was ground and passed through sieves leaving fractions of <20, 20−40, and 50−80 μm. Figure 6 depicts the TG curves and DTA measurements of the reactions of these fractions with pure oxygen. Mass increase due to formation of Sc_2O_3 significantly starts as low as T = 710 K. Increasing rates of oxidation are apparent above T = 970 K, as might be expected faster and at lower temperatures for the smaller particle sizes. Interestingly, the DTA displays two exothermic maxima. A possible explanation assigns one maximum to the oxidation of smaller particle sizes (T_{max} = 1050 K) and assigns the second one to the oxidation of the larger particles (T_{max} = 1150 K), possibly due to different particle morphologies.

In the literature most polycrystalline bulk samples of ScN_x are described as gray or black powders, while the red color of ScN obtained from a molecular precursor at comparatively low temperatures (673 K)[7] corresponds well with the reported band gap of ΔE = 2.1 eV.[6,36] According to band structure calculations ScN exhibits an indirect band gap,[37] thus it is not surprising that different authors could not extract a band gap from their optical data.[38] Our measurements of diffuse scattering on polycrystalline bulk samples result in an absorption edge at ΔE = 2.10(2) eV consistent with the brownish color of the freshly ground powder and the translucent brown single crystals. In accordance with these results magnetic susceptibility measurements indicate only a small amount of paramagnetic impurities (corresponding to about 1×10^{-3} of spin 1/2 ions) and a temperature independent paramagnetism of about $\chi_0 = 2.7-5.6 \times 10^{-6}$ emu/mol. With increasing particle size these values decrease, which might be associated with a smaller degree of defects in the larger particles (esp. in the single crystals, $\chi_0 = 2.7 \times 10^{-6}$ emu/mol). Still, electrical resistivity measurements on a single crystal show a metal-like behavior with $\rho(300\ \text{K}) = 2.1 \times 10^{-4}$ Ωcm, $\rho_0 = 1.0 \times 10^{-4}$ Ωcm, and a temperature coefficient of $\alpha = 2.7 \times 10^{-3}\ \text{K}^{-1}$ around 300 K (Figure 7). These results agree well with data obtained on sintered polycrystalline materials measured in the range of 80−500 K ($\rho = 1.3 \times 10^{-4}$ Ωcm, $\alpha = 1.5 \times 10^{-3}\ \text{K}^{-1}$).[38] Even though we are dealing with samples close to the composition ScN the remaining defects are sufficient to convert the 2 eV insulator into a heavily doped defect-type semiconductor (i.e., with constant charge carrier concentration over a

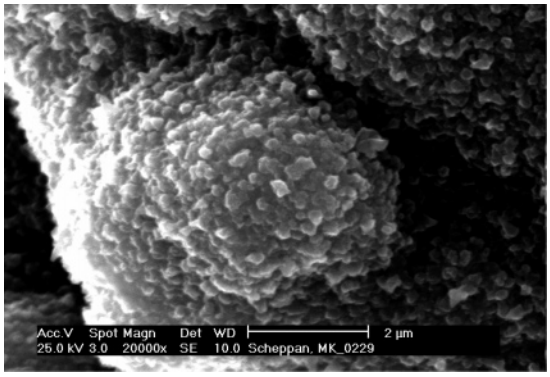

Figure 5. Scanning electron microscopy representation of ScN particles obtained from reaction of Sc_2In with N_2.

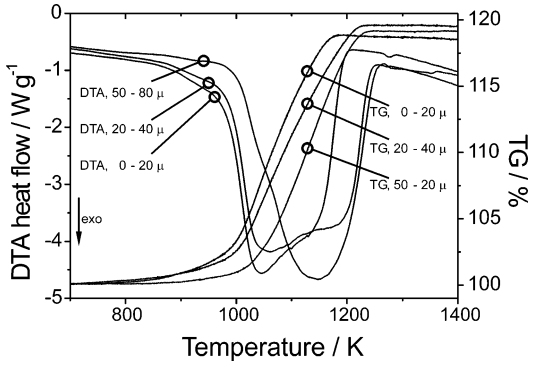

Figure 6. DTA/TG diagrams of the reaction of ScN in O_2-atmosphere depending on the particle size (heating rate 10 K/min).

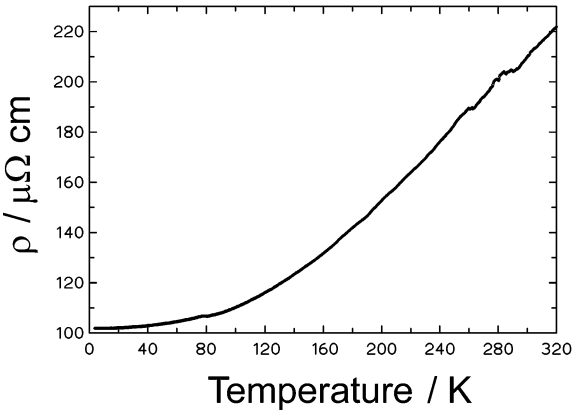

Figure 7. Electrical resistivity of a ScN crystal plotted as function of the temperature.

large temperature range). This is explained by the simple fact that even 1% defects in the N-sublattice (i.e., $ScN_{0.99}$) may already account for an order of magnitude of 10^{21} charge carriers/cm^3.

4. Conclusion

High-quality bulk ScN was obtained by a variety of preparation techniques, optimized for single crystals and for small particle sizes. ScN represents an oxidation-resistant intrinsic semiconductor, however, it shows impurity-based metal-like electrical resistivity.

Acknowledgment. We thank Steffen Hückmann and Dr. Huiqiu Yuan for collection of the X-ray diffraction data, Ulrike Schmidt and Britta Bayer for performing the chemical analyses, Dr. Ulrich Burkhardt for density measurements, and Dr. Ulrich Schwarz for measurement of the diffuse reflectance data. Petra Scheppan is acknowledged for the SEM images and Prof. Rüdiger Kniep is acknowledged for his constant interest and support. We also thank Prof. Heinrich Oppermann for valuable discussions on the thermodynamic considerations.

CM048667Y